ISSN 1070-3284, Russian Journal of Coordination Chemistry, 2018, Vol. 44, No. 12, pp. 792–799. © Pleiades Publishing, Ltd., 2018.

Syntheses, Structures, and Luminescent Properties of Two Alkaline Earth Metal Coordination Polymers from Hydroxymethyl Imidazole Dicarboxylate[1]

G. Chen[a], H. H. Lan[a], Z. X. Li[a], D. J. Li[a], G. J. Peng[a], S. L. Cai[a, *], S. R. Zheng[a, **], and W. G. Zhang[a]

[a] *School of Chemistry and Environment, South China Normal University, Guangzhou, 510006 P.R. China*

**e-mail: songliangcai@m.scnu.edu.cn*

***e-mail: zhengsr@scnu.edu.cn*

Received April 26, 2018

Abstract—Two new alkaline earth metal coordination polymers, which are $[Ba(H_2IDC)(H_3HmIDC)(H_2O)_2]_n$ (**I**) and $[Sr(H_2HmIDC)]_n$ (**II**) [H_3IDC = 1*H*-imidazole-4,5-dicarboxylic acid, H_4HmIDC = 2-(hydroxymethyl)-1*H*-imidazole-4,5-dicarboxylic acid), respectively, have been successfully synthesized under solvothermal conditions by employing H_4HmIDC as the starting material. Both compounds **I** and **II** were structurally characterized by diverse techniques, such as single crystal X-ray diffraction (CIF files CCDC nos. 1839705 (**I**) and 1839706 (**II**)), FT-IR spectra, powder X-ray diffraction, and thermogravimetric analyses. Compound **I** exhibits a two-dimentional (2D) coordination network with a (4, 4) topology based on dinuclear $[Ba_2O_4]$ as second building units (SBUs). Whereas compound **II** features a 3D coordination framework based on infinite 1D inorganic chains as SBUs, which can be further simplified as a 5-connected noy topology. In addition, the photoluminescent properties of both compounds **I** and **II** were also investigated.

Keywords: imidazole-4,5-dicarboxylate, alkaline earth metal coordination polymer, luminescent property

DOI: 10.1134/S1070328418120023

INTRODUCTION

Over the past decade, the construction of metal coordination polymers by using H_3IDC (H_3IDC = 1*H*-imidazole-4,5-dicarboxylic acid) [1–8] or functionalized H_3IDC, including 2-(hydroxymethyl)-1*H*-imidazole-4,5-dicarboxylic acid (H_4HmIDC) [9–32] as multidentate ligands has received much attention. The main reason is due to the fact that these coordination polymers not only exhibit fascinating frameworks and interesting topologies, but also show promising applications in the areas of gas absorption [1–5], magnetic material [6–10], chemical sensor [11–15], and so forth. It has been found that both H_3IDC and its derivatives having diverse substituents at 2-position of the imidazole ring can coordinate with different types of metal ions in various coordination modes by taking advantage of the strong coordination abilities of four carboxylate oxygen atoms or/and imidazole nitrogen atoms, therefore creating a variety of new coordination polymers with structural diversity [1–32].

In 2011, our group has firstly designed and prepared a new functionalized H_3IDC ligand [33] through the introduction of a hydroxymethyl group into the 2-position of the parent H_3IDC. The coordination chemistry of H_4HmIDC ligand has aroused our interest due to the different reaction behaviors of the introduced hydroxymethyl group under appropriate conditions. Firstly, the hydroxymethyl group can bond to metal ions to construct more complicated coordination polymers with higher dimensionality [33–36]. Secondly, it also may remain uncoordinated and act as hydrogen bonding donor or acceptor to form hydrogen bonds like O–H···O and O–H···N, which are beneficial for the construction of various supramolecular architectures [33, 36]. More importantly, the introduced hydroxymethyl group can undergo *in situ* reactions, such as dehydroxymethylation reaction [37] and oxidation of hydroxymethyl group to carboxyl group [33], thus resulting in the formation of some unprecedented coordination polymers with interesting properties.

As a continuing investigation, in the present work, we report the solvothermal syntheses and crystal structures of two new alkaline earth metal coordination polymers formulated as $[Ba(H_2IDC)(H_3HmIDC)(H_2O)_2]_n$ (**I**) and $[Sr(H_2HmIDC)]_n$ (**II**), respectively, by utilizing H_4HmIDC as the starting reactant. Interestingly, part of H_4HmIDC ligand has

[1] The article is published in the original.

been convered to H_3IDC via *in situ* dehydroxymethylation reaction in compound **I**, which gives rise to a 2D coordination network, while the hydroxymethyl group of H_4HmIDC in compound **II** has participated in coordinating with Sr^{2+} ion to produce a complicated 3D framework. Additionally, the FT-IR spectra, powder X-ray diffraction (PXRD) measurements and thermogravimetric (TG) curves, as well as solid-state luminescence properties of both two compounds have been also studied and discussed in detail in the text.

EXPERIMENTAL

Materials and measurements. The ligand H_4HmIDC was synthesized based on the procedure we previously employed [33]. All the other chemicals were of analytical grade quality, which could be bought from commercial vendors and were used as received directly. FT-IR spectra were carried out on a Nicolet FT-IR-170SX spectrophotometer in the region of 4000–400 cm^{-1} utilizing KBr pellet. PXRD patterns were measured in the 2θ range of 5°–50° with recording speed of 5°/min on a Bruker D8 Advance diffractometer at 40 kV, 40 mA by using CuK_α radiation (λ = 1.5418 Å). TG analyses were determined by employing a Netzsch STA409PC Thermal Analyzer with a ramp rate of 10°C/min in flowing air atmosphere. Solid-state fluorescence spectra were performed on a Hitachi F-4500 fluorescence spectrophotometer at room temperature with a 150 W xenon lamp as the light source.

Synthesis of compound I. A mixture of H_4HmIDC (37.2 mg, 0.20 mmol), $BaCl_2 \cdot 2H_2O$ (48.9 mg, 0.2 mmol), $AgNO_3$ (34.0 mg, 0.2 mmol), 6 mL EtOH–H_2O (1 : 1 by volume), and Et_3N (0.15 mL) was sealed in a 15 mL Teflon-lined stainless steel autoclave, heated at 130°C for 72 h, and then slowly cooled to room temperature at a rate of 2°C/h. Pink block-shaped crystals of **I** were obtained in a yield of 37% (based on the Ba) after washing with EtOH and drying in air.

IR (KBr; ν, cm^{-1}): 3565 m, 3130 s, 2958 w, 2926 w, 1853 w, 1592 s, 1558 s, 1526 m, 1428 m, 1381s, 1249 s, 1121 w, 1083 w, 1065 w, 1021 m, 950 w, 858 w, 813 w, 780 w, 662 w, 639 w, 611 w, 526 w, 515 w, 436 w.

Synthesis of compound II. H_4HmIDC (37.2 mg, 0.20 mmol) and $Sr(NO_3)_2$ (42.4 mg, 0.20 mmol) were mixed in 6 mL EtOH–H_2O (1 : 1 by volume) and the pH was adjusted to about 2 by the slow addition of the aqueous HNO_3 solution. The resulting mixture was transferred into a 15 mL Teflon-lined stainless steel autoclave, heated at 170°C for 72 h under autogenous pressure, and finally cooled to room temperature at a rate of 3°C/h. Pale-yellow block-like crystals of **II** were collected, washed with EtOH and dried in air, giving a yield of 58% (based on H_4HmIDC).

IR (KBr; ν, cm^{-1}): 3135 w, 3088 w, 3038 w, 2978 w, 2862 s, 1586 s, 1562 s, 1519 m, 1461 m, 1410 w, 1382 s, 1360 s, 1249 w, 1105 w, 1056 m, 1018 w, 963 w, 864 w, 836 w, 798 w, 760 w, 730 w, 679 w, 654 w, 615 w, 535 m, 413 w.

X-ray crystallography. Single-crystal X-ray diffraction data collection for the compounds **I** and **II** were conducted on a Bruker APEX II diffractometer employing graphite-monochromated MoK_α radiation (λ = 0.71073 Å) at 298(2) K. Data reduction and absorption correction for both two structures were performed by utilizing the Bruker SAINT and SADABS programs [38], respectively. While their structural solutions and full-matrix least-squares refinements based on F^2 were performed with the SHELXS-2014 and SHELXL-2014 crystallographic software packages [39, 40], respectively. All of the non-hydrogen atoms were found from the difference Fourier maps and refined with anisotropic thermal displacement parameters. And the hydrogen atoms on the organic ligands were generated geometrically and refined isotropically using the riding model. Further details of the crystal parameters, data collections, and structural refinements for the compounds **I** and **II** are summarized in Table 1, and selected bond distances and angles with their estimated standard deviations are presented in Table 2. Crystallographic data for **I** and **II** have been deposited with the Cambridge Crystallographic Data Centre (CCDC nos. 1839705 and 1839706 for **I** and **II**, respecitively; www.ccdc.cam.ac.uk/data_request/cif).

RESULTS AND DISCUSSION

Single crystal structure determination indicates that compound **I** exhibits a 2D coordination framework consisting of dinuclear $[Ba_2O_4]$ second building units (SBUs). There are only one crystallographically independent Ba^{2+} ion, a H_3HmIDC^- anion and a H_2IDC^- anion, as well as two coordinated water molecules in asymmetric unit of compound **I**. Notably, part of the H_4HmIDC ligand has been converted into the H_3IDC ligand through in situ dehydroxymethylation during the solvothermal conditions, thereby generating the H_2IDC^- anion. As presented in Scheme 1a and 1b, the H_2IDC^- and the H_3HmIDC^- ligands act as the bidentate ligands to connect with two Ba^{2+} ions, but in slightly different coordination modes: the former one adopts a μ_2-kO:kO' coordination fashion, while the later one employs a μ_2-kO,N:kO' coordination mode. The two coordinated water molecules also adopt different coordination behaviors, one of them acts as a terminal ligand, while the other serves as a μ_2-bridge ligand. The coordination environment of the central Ba^{2+} ion is illustrated in Fig. 1a. Each Ba(II) atom is nine-coordinated with a distorted $[BaNO_8]$ geometry, being surrounded by three carboxylate oxygen atoms and one imidazole nitrogen atom from three different μ_2-H_3HmIDC^- ligands, and

Table 1. Crystallographic data and structure refinements for compounds **I** and **II**

Parameter	Value	
	I	**II**
Empirical formula	$C_{11}H_{12}N_4O_{11}Ba$	$C_6H_4N_2O_5Sr$
Formula weight	513.59	271.73
Crystal system	Orthorhombic	Monoclinic
Space group	*Pbca*	$P2_1/c$
a, Å	14.0201(16)	6.6185(12)
b, Å	12.8179(14)	15.923(3)
c, Å	17.2941(19)	7.0790(13)
β, deg	90	94.752(2)
V, Å^3	3107.9(6)	743.5(2)
Z	8	4
ρ_{calcd}, mg m^{-3}	2.195	2.428
μ, mm^{-1}	2.631	7.249
F(000)	2000	528
θ Range for data collection, deg	2.355–26.999	2.558–25.996
Max, min transmission	0.7456, 0.4984	0.7456, 0.4383
Reflections collected	16 992	4013
Unique reflections	3391	1462
Reflections with $I > 2\sigma(I)$	3071	1171
R_{int}	0.0277	0.0393
R_1*, wR_2** ($I > 2\sigma(I)$)	0.0331, 0.0773	0.0364, 0.0861
R_1*, wR_2** (all data)	0.0373, 0.0792	0.0516, 0.0943
Goodness-of-fit on F^2	1.096	1.021
$\Delta\rho_{max}$ and $\Delta\rho_{min}$, *e* Å^{-3}	1.749/–0.732	1.271/–0.785

* $R_1 = \Sigma||F_o| - |F_c||/\Sigma|F_o|$, ** $wR_2 = \{\Sigma[w(F_o^2 - F_c^2)^2]/\Sigma(F_o^2)^2\}^{1/2}$.

two carboxylate oxygen atoms from two individual μ_2-H_2IDC^- ligands, as well as one terminal and two μ_2-bridge H_2O ligands. As listed in Table 2, the Ba–N bond length is 2.914(3) Å, which is longer than those of Ba–O distances (2.717(3)–2.887(3) Å). Whereas the bond angles around the central Ba^{2+} ion span from 57.17(8)° to 152.09(9)°. All of the above bond lengths and angles are comparable to those observed for the other nine-coordinated Ba(II) coordination polymers assembled from imidazole-based dicarboxylic acid ligands [26, 36].

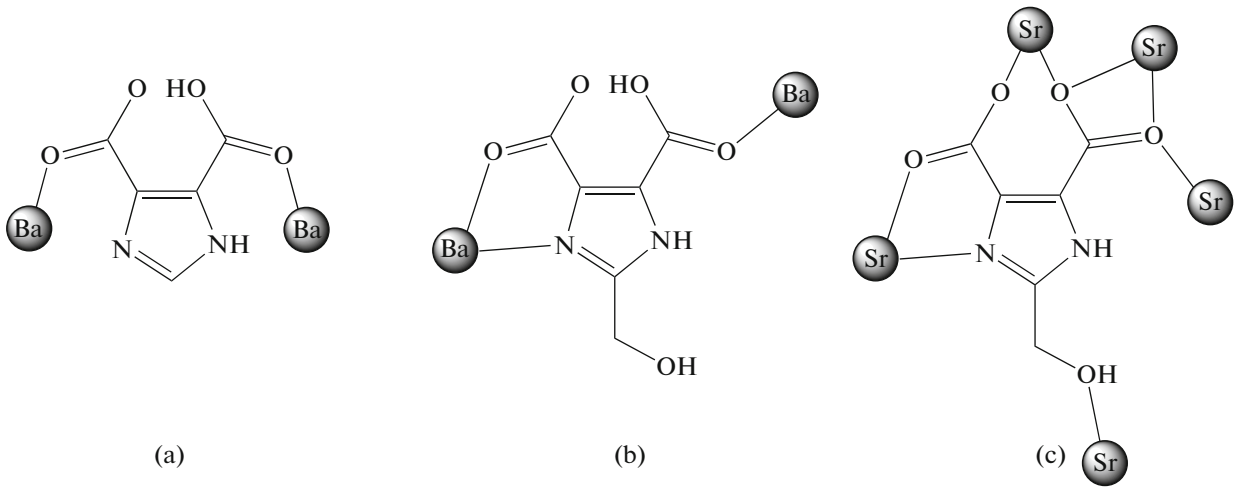

Scheme 1.

Table 2. Selected bond lengths (Å) and angles (deg) for compounds **I** and **II***

Bond	*d*, Å	Bond	*d*, Å	Bond	*d*, Å
		I			
Ba(1)–O(1)	2.717(3)	Ba(1)–O(6)	2.737(3)	Ba(1)–O(2*w*)	2.821(4)
Ba(1)–O(1*w*)$^{\#1}$	2.828(3)	Ba(1)–O(1*w*)	2.838(3)	Ba(1)–O(4)$^{\#2}$	2.871(3)
Ba(1)–O(9)$^{\#2}$	2.874(3)	Ba(1)–O(4)$^{\#3}$	2.887(3)	Ba(1)–N(2)$^{\#3}$	2.914(3)
		II			
Sr(1)–O(4)$^{\#1}$	2.476(3)	Sr(1)–O(3)$^{\#4}$	2.614(4)	Sr(1)–N(1)$^{\#2}$	2.741(4)
Sr(1)–O(1)$^{\#2}$	2.479(3)	Sr(1)–O(2)$^{\#4}$	2.643(3)	Sr(1)–O(4)$^{\#3}$	2.828(3)
Sr(1)–O(3)$^{\#3}$	2.591(4)	Sr(1)–O(5)	2.676(4)		
Angle	ω, deg	Angle	ω, deg	Angle	ω, deg
		I			
O(1)Ba(1)O(6)	72.90(10)	O(2*w*)Ba(1)O(4)$^{\#2}$	134.94(12)	O(1*w*)$^{\#1}$Ba(1)O(4)$^{\#3}$	57.65(8)
O(1)Ba(1)O(2w)	135.02(12)	O(1*w*)$^{\#1}$Ba(1)O(4)$^{\#2}$	61.87(8)	O(1*w*)Ba(1)O(4)$^{\#3}$	61.57(8)
O(6)Ba(1)O(2*w*)	62.38(12)	O(1*w*)Ba(1)O(4)$^{\#2}$	57.74(8)	O(4)$^{\#2}$Ba(1)O(4)$^{\#3}$	90.45(8)
O(1)Ba(1)O(1*w*)$^{\#1}$	136.04(9)	O(1)Ba(1)O(9)$^{\#2}$	83.90(9)	O(9)$^{\#2}$Ba(1)O(4)$^{\#3}$	132.51(8)
O(6)Ba(1)O(1*w*)$^{\#1}$	132.80(10)	O(6)Ba(1)O(9)$^{\#2}$	72.18(9)	O(1)Ba(1)N(2)$^{\#3}$	105.14(9)
O(2*w*)Ba(1)O(1*w*)$^{\#1}$	78.28(12)	O(2*w*)Ba(1)O(9)$^{\#2}$	78.46(11)	O(6)Ba(1)N(2)$^{\#3}$	85.13(9)
O(1)Ba(1)O(1*w*)	74.86(9)	O(1*w*)$^{\#1}$Ba(1)O(9)$^{\#2}$	75.44(8)	O(2*w*)Ba(1)N(2)$^{\#3}$	76.67(12)
O(6)Ba(1)O(1*w*)	138.59(10)	O(1*w*)Ba(1)O(9)$^{\#2}$	128.94(9)	O(1*w*)$^{\#1}$Ba(1)N(2)$^{\#3}$	111.26(8)
O(2*w*)Ba(1)O(1*w*)	145.65(10)	O(4)$^{\#2}$Ba(1)O(9)$^{\#2}$	72.19(8)	O(1*w*)Ba(1)N(2)$^{\#3}$	78.91(9)
O(1*w*)$^{\#1}$Ba(1)O(1*w*)	88.59(9)	O(1)Ba(1)O(4)$^{\#3}$	134.83(9)	O(4)$^{\#2}$Ba(1)N(2)$^{\#3}$	135.43(9)
O(1)Ba(1)O(4)$^{\#2}$	75.05(9)	O(6)Ba(1)O(4)$^{\#3}$	135.56(8)	O(9)$^{\#2}$Ba(1)N(2)$^{\#3}$	152.09(9)
O(6)Ba(1)O(4)$^{\#2}$	133.85(8)	O(2*w*)Ba(1)O(4)$^{\#3}$	84.83(10)	O(4)$^{\#3}$Ba(1)N(2)$^{\#3}$	57.17(8)
		II			
O(4)$^{\#1}$Sr(1)O(1)$^{\#2}$	81.29(11)	O(4)$^{\#1}$Sr(1)O(5)	73.34(12)	O(5)Sr(1)N(1)$^{\#2}$	85.37(11)
O(4)$^{\#1}$Sr(1)O(3)$^{\#3}$	123.60(11)	O(1)$^{\#2}$Sr(1)O(5)	79.99(11)	O(4)$^{\#1}$Sr(1)O(4)$^{\#3}$	76.04(12)
O(1)$^{\#2}$Sr(1)O(3)$^{\#3}$	151.69(11)	O(3)$^{\#3}$Sr(1)O(5)	93.75(12)	O(1)$^{\#2}$Sr(1)O(4)$^{\#3}$	152.06(11)
O(4)$^{\#1}$Sr(1)O(3)$^{\#4}$	129.84(13)	O(3)$^{\#4}$Sr(1)O(5)	154.79(11)	O(3)$^{\#3}$Sr(1)O(4)$^{\#3}$	47.59(10)
O(1)$^{\#2}$Sr(1)O(3)$^{\#4}$	110.37(12)	O(2)$^{\#4}$Sr(1)O(5)	141.57(11)	O(3)$^{\#4}$Sr(1)O(4)$^{\#3}$	96.73(11)
O(3)$^{\#3}$Sr(1)O(3)$^{\#4}$	65.99(14)	O(4)$^{\#1}$Sr(1)N(1)$^{\#2}$	140.89(11)	O(2)$^{\#4}$Sr(1)O(4)$^{\#3}$	112.93(11)
O(4)$^{\#1}$Sr(1)O(2)$^{\#4}$	74.10(12)	O(1)$^{\#2}$Sr(1)N(1)$^{\#2}$	62.63(10)	O(5)Sr(1)O(4)$^{\#3}$	78.04(11)
O(1)$^{\#2}$Sr(1)O(2)$^{\#4}$	75.42(11)	O(3)$^{\#3}$Sr(1)N(1)$^{\#2}$	89.49(11)	N(1)$^{\#2}$Sr(1)O(4)$^{\#3}$	131.70(11)
O(3)$^{\#3}$Sr(1)O(2)$^{\#4}$	121.36(12)	O(3)$^{\#4}$Sr(1)N(1)$^{\#2}$	79.86(12)		
O(3)$^{\#4}$Sr(1)O(2)$^{\#4}$	63.26(11)	O(2)$^{\#4}$Sr(1)N(1)$^{\#2}$	108.18(11)		

* Symmetry transformations used to generate equivalent atoms: $^{\#1}$ $-x+1, -y+1, -z+2$; $^{\#2}$ $x-1/2, y, -z+3/2$; $^{\#3}$ $-x+3/2, -y+1, z+1/2$ for **I**; $^{\#1}$ $x, -y+3/2, z+1/2$; $^{\#2}$ $x-1, y, z$; $^{\#3}$ $-x+1, y-1/2, -z+1/2$; $^{\#4}$ $x-1, -y+3/2, z+1/2$ for **II**.

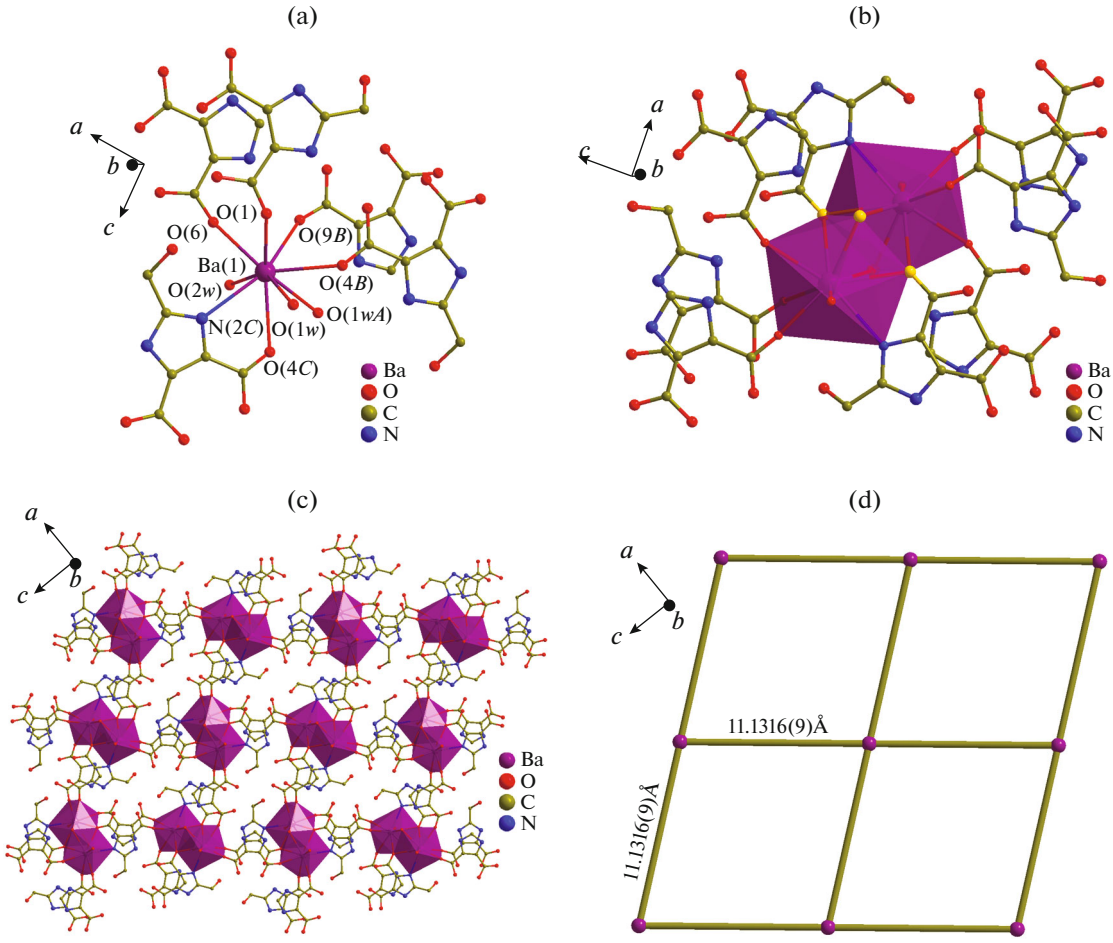

Fig. 1. The coordination geometry around Ba $^{2+}$ ions in **I** (the hydrogen atoms are omitted for clarity; symmetry codes: (*A*) $-x+1, -y+1, -z+2$; (*B*) $x-1/2, y, -z+3/2$; (*C*) $-x+3/2, -y+1, z+1/2$) (a); the dinuclear $[Ba_2O_4]$ SBU in compound **I** (the O(4) and O(1*w*) atoms showing the μ_2-bridge mode are highlighted in gold) (b); the 2D coordination framework of compound **I** extending along the *ac* plane (c); the (4, 4) topological network in compound **I** (d).

In compound **I**, two crystallographically equivalent Ba^{2+} ions the are bridged by two oxygen atoms from the H_2O ligands (O(1*w*) and O(1*wA*), symmetry codes: (*A*) $-x+1, -y+1, -z+2$) and two carboxylate oxygen atoms from the H_2IDC^- ligands (O(4*B*) and O(4*C*), symmetry codes: (*B*) $x-1/2, y, -z+3/2$; (*C*) $-x+3/2, -y+1, z+1/2$) by using the μ_2-bridge mode, giving rise to the formation of a binuclear $[Ba_2O_4]$ SBU, as shown in Fig. 1b. In such a $[Ba_2O_4]$ dimer, the separation distance of Ba...Ba is 4.0553(5) Å. Moreover, every binuclear $[Ba_2O_4]$ SBU connects to four other neighbouring SBUs through four μ_2-H_2IDC^- ligands and four μ_2-H_3HmIDC^- ligands, thus leading to the construction of a 2D coordination framework extending along the *ac* plane, as described in Fig. 1c. From a topological viewpoint, if each binuclear $[Ba_2O_4]$ SBU is considered as a 4-connected node, the resulting 2D layered structure of compound **I** can be a (4, 4) topological network, as depicted in Fig. 1d.

Compound **II** belongs possesses a 3D coordination framework based on infinite 1D chains as SBUs. The related asymmetric unit of this compound comprises only one crystallographically independent Sr(II) cation and one H_2HmIDC^{2-} anion. As described in Fig. 2a, the Sr^{2+} ion is eight-coordinated with six carboxylate oxygen atoms, one hydroxymethyl oxygen atom and one imidazole nitrogen atom from five individual H_2HmIDC^{2-} anions, giving rise to a distorted bicapped trigonal prism $[SrNO_7]$ coordination environment. The Sr–N bond length is 2.741(4) Å, and the Sr–O bond distances are in the scope of 2.476(3)–2.828(3) Å, while the bond angles around Sr^{2+} ion span from 47.59(10)° to 154.79(11)°, all of which fall in the normal range.

In compound **II**, each doubly deprotonated H_2HmIDC^{2-} ligand adopts a complicated coordination fashion which is μ_5-kN,O:kO',O":kO":kO"':kO"" to connect five crystallographically equivalent Sr^{2+} ions in N,O-chelating, O',O"-chelating, O"-bridging,

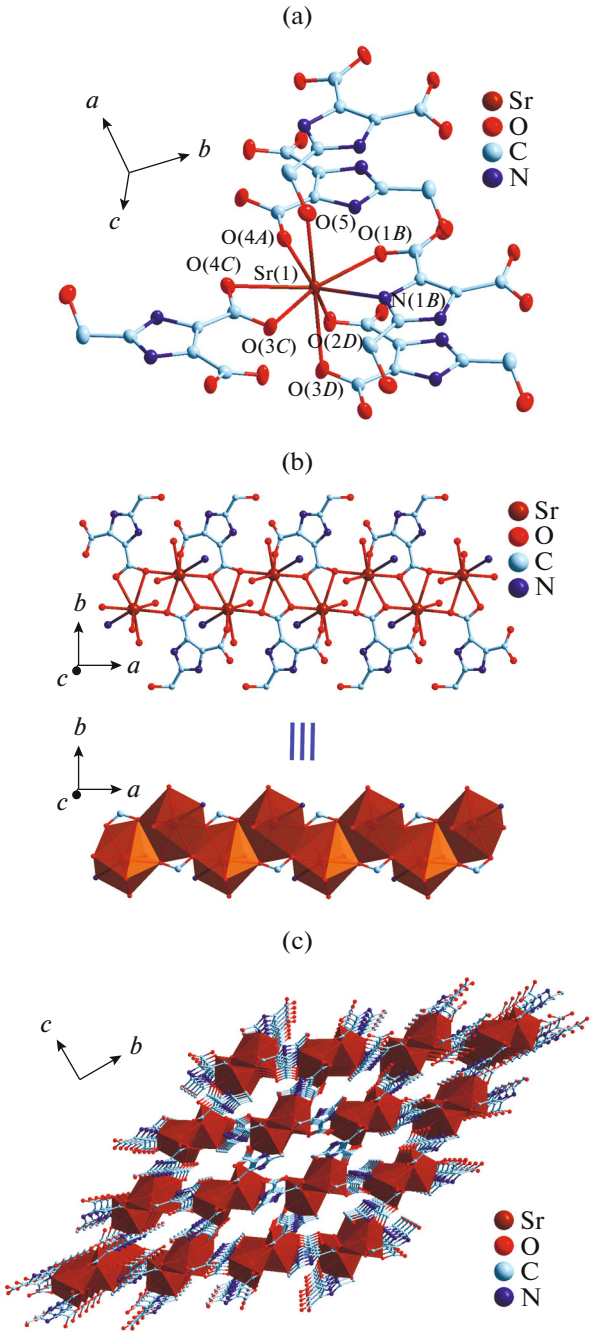

Fig. 2. The coordination environment of Sr^{2+} ion in **II** (the hydrogen atoms are omitted for clarity; symmetry codes: (*A*) $x, -y + 3/2, z + 1/2$; (*B*) $x - 1, y, z$; (*C*) $-x + 1, y - 1/2, -z + 1/2$; (*D*) $x - 1, -y + 3/2, z + 1/2$) (a); ball-and-stick and polyhedral view of the 1D SBU in compound **II** (b); the 3D coordination framework of **II** based on 1D SBUs (c).

and monodentate modes, as displayed in Scheme 1c. Such a coordination mode is the same to that of our previously reported alkaline earth metal coordination polymer derived from H_4HmIDC ligand [36]. It is worth noting that one of the carboxylate groups from the H_2HmIDC^{2-} ligand empolys a μ_3-η^2:η^1 coordination fashion to alternately bridge the neighbouring Sr^{2+} ions, resulting in the formation of an infinite 1D inorganic chain running along the *a* axis (Fig. 2b). The adjacent nonbonding Ba···Ba distances in such a 1D inorganic chain are 4.1843(8) and 4.3651(8) Å, respectively. Moreover, these 1D chains which can be seen as 1D SBUs are further connected each other via the μ_5-H_2HmIDC^{2-} ligand in different orientation, thereby creating a 3D coordination framework as presented in Fig. 2c.

The topological analysis approach, which usually can be seen as a standard procedure for reducing multidimensional structures to a simple node-and-linker, was used to better describe and understand the whole structure of compound **II**. As discussed above, both the μ_5-H_2HmIDC^{2-} ligand and Sr(II) center can be denoted as five-connected nodes (Fig. 3a) with the same vertex symbol of $(4 \cdot 4 \cdot 4 \cdot 4 \cdot 4 \cdot 4 \cdot 6_2 \cdot 6_2 \cdot 6_2 \cdot 6_2)$. In consequence, the resulting structure of compound **II** can be simplified as a five-connected **noy** type 3D framework, and the coresponding Schläfli symbol of this framework is $(4^6 \cdot 6^4)$ as analyzed by TOPOS program (Fig. 3b) [41].

The IR spectrum of compound **I** has some broad absorption peaks in the range of 3650–3000 cm^{-1}, which probably can be attributable to the characteristic peaks of O–H stretching modes from the coordinated water molecules and the hydroxymethyl group of the H_3HmIDC^- ligand, as well as the N–H vibrations from the imidazole rings of the H_2IDC^- and H_3HmIDC^- ligands. While for compound **II**, its IR spectrum also shows broad absorption bands spanning from 3400 to 2950 cm^{-1}, corresponding to the O–H and N–H stretching vibrations from the hydroxymethyl and imidazole groups of the H_2HmIDC^{2-} ligand. Besides, intense bands around 1610–1540 and 1400–1340 cm^{-1} can be observed in the spectra of both two compounds, which may be assigned to the asymmetric stretches (ν_{as}) and symmetric stretches (ν_s) from the carboxylate groups of the organic ligands, respectively [42]. In short, the IR spectral data of compounds **I** and **II** are quite consistent with their X-ray single-crystal structures.

For purpose of confirming the phase purity of the as-prepared bulky crystalline samples, PXRD experiments for compounds **I** and **II** have been conducted. The PXRD patterns of compounds **I** and **II** measured at room temperature match pretty well with those generated from X-ray single crystal diffraction data in terms of the peak positions, which obviously suggests the crystalline phase homogeneity of both two compounds. It's necessary to note that the dissimilarities in reflection intensity between the measured patterns and the simulated ones may be due to the preferred orientation of the powder samples during the collection of the PXRD data.

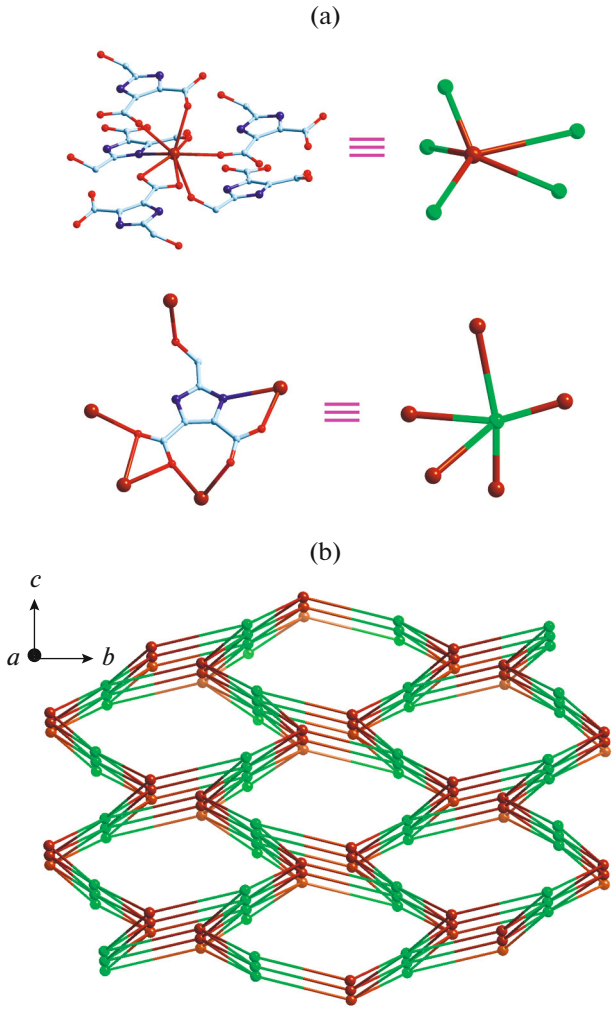

Fig. 3. The five-connected nodes of Sr^{2+} metal center and H_2HmIDC^{2-} ligand center in compound **II** (a); the five-connected network topology of compound **II** (b).

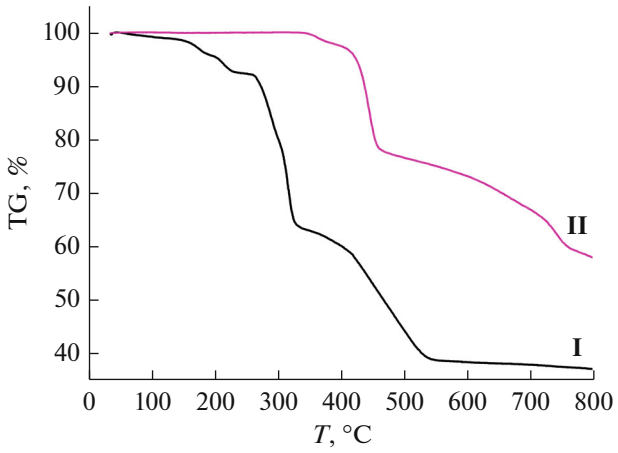

Fig. 4. The TGA curves for the compounds **I** and **II**.

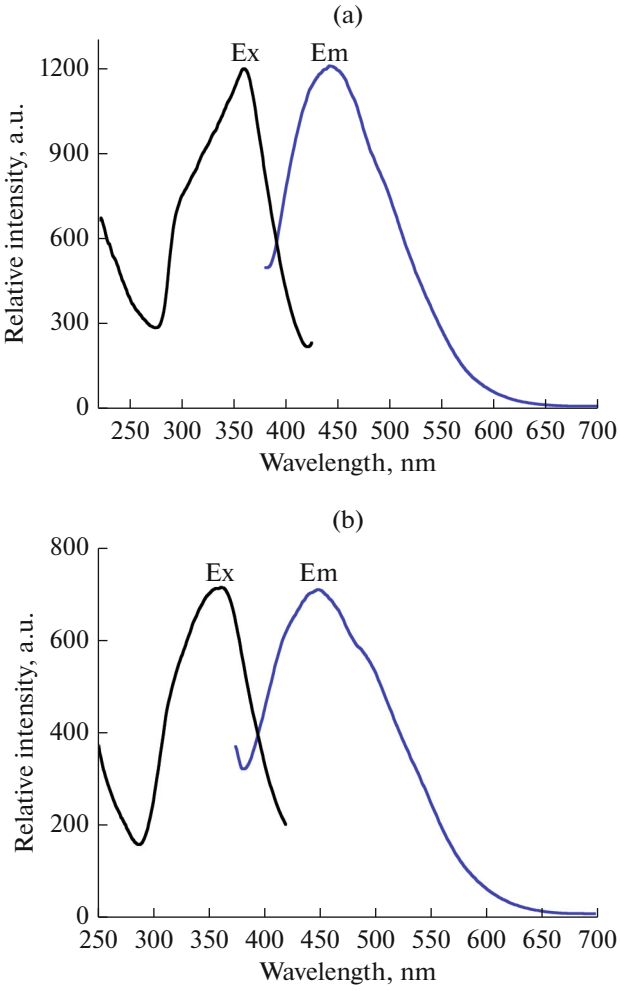

Fig. 5. The solid state excitation and emission spectra of compound **I** (a) and compound **II** (b) at room temperature.

In order to check the thermal stabilities of the coordination frameworks, TG analyses of compounds **I** and **II** were carried out from room temperature to 800°C under air atmosphere with a heating rate of 10°C min^{-1}, and the corresponding TG curves are shown in Fig. 4. For compound **I**, the initial weight loss of 7.2% from room temperature to 230°C can be ascribed to the gradual departure of two coordination water molecules in the asymmetric unit (calcd. 7.0%). Such a solvent-free framework of compound **I** is thermally stable up to about 260°C, and further increasing the temperature results in the decomposition of the H_2IDC^- and H_3HmIDC^- ligands as well as the collapse of the whole framework structure. In case of compound **II**, due to the fact that no coordinated or guest solvent molecule can be found in the crystal structure, thus its TG curve exhibits no obvious weight loss before the temperature of 340°C. The 3D coordination framework of **II** can just be thermally stable to

340°C, and it starts to decompose when further raising the temperature.

On the basis of the previously reported literature, the luminescent properties of alkaline earth metal coordination polymers are not well investigated when compared with those of lanthanide or transition metal coordination polymers. Therefore, the photoluminescent properties of compounds **I** and **II** have been studied in the solid state at ambient temperature, and the results are illustrated in Fig. 5. Both compounds **I** and **II** display blue photoluminescence with the maximum emission wavelengths appeared at 442 and 449 nm upon excitation at 366 and 362 nm, respectively. The free H_3IDC and H_4HmIDC ligands exhibit fluorescent emission bands centered at 410 nm (when excited between 280 and 480 nm) [43] and 461 nm (when excited at 370 nm) [36], respectively, based on the literature. Compared with the free ligands, the emission bands of compounds **I** and **II** can probably be attributable to the intra-ligand $\pi-\pi^*$ transitions since both the alkaline earth metal ions Ba^{2+} and Sr^{2+} are generally considered to be difficult to oxidize or reduce [36].

ACKNOWLEDGMENTS

This work was fnancially supported by the National Natural Science Foundation of P.R. China (grant nos. 21603076, 21571070 and 21473062), the Natural Science Foundation of Guangdong Province (grant nos. 2016A030310437 and 2018A030313193), and the Undergraduates' Innovating Experimentation Project of SCNU and Guangdong Province (grant no. 20181462).

REFERENCES

1. Maji, T.K., Mostafa, G., Chang, H.C., and Kitagawa, S., *Chem. Commun.*, 2005, p. 2436.
2. Liu, Y., Kravtsov, V.C., Larsen, R., and Eddaoudi, M., *Chem. Commun.*, 2006, p. 1488.
3. Gurunatha, K.L., Uemura, K., and Maji, T.K., *Inorg. Chem.*, 2008, vol. 47, p. 6578.
4. Gu, Z.G., Cai, Y.P., Fang, H.C., et al., *Chem Commun.*, 2010, vol. 46, p. 5373.
5. Peralta, D., Chaplais, G., Simon-Masseron, A., et al., *J. Am. Chem. Soc.*, 2012, vol. 134, p. 8815.
6. Wang, C.F., Gao, E.Q., He, Z., and Yan, C.H., *Chem. Commun.*, 2004, p. 720.
7. Xu, Q., Zou, R.Q., Zhong, R.Q., et al., *Cryst. Growth Des.*, 2008, vol. 8, p. 2458.
8. Cruz, C., Spodine, E., Vega, A., et al., *Cryst. Growth Des.*, 2016, vol. 16, p. 2173.
9. Cai, S.L., Zheng, S.R., Wen, Z.Z., et al., *Cryst. Growth Des.*, 2012, vol. 12, p. 4441.
10. Zhang, X.J., Liu, K., Bing, Y.M., et al., *Dalton Trans.*, 2015, vol. 44, p. 7757.
11. Cai, S.L., Zheng, S.R., Fan, J., et al., *Inorg. Chem. Commun.*, 2011, vol. 14, p. 937.
12. Yue, Z.F., Chen, Z.N., Yao, M.J., et al., *RSC Adv.*, 2014, vol. 4, p. 33537.
13. Shi, B.B., Zhong, Y.H., Guo, L.L., and Li, G., *Dalton Trans.*, 2015, vol. 44, p. 4362.
14. Li, Y.L., Wang, J., Shi, B.B., and Li, J.P., *Supramol. Chem.*, 2016, vol. 28, p. 640.
15. Huang, Q.Y., Zhao, Y., Fu, L., and Li, G., *Russ. J. Coord. Chem.*, 2017, vol. 43, p. 604. doi 10.1134/S1070328417090032
16. Li, X., Wu, B.L., Niu, C.Y., et al., *Cryst. Growth Des.*, 2009, vol. 9, p. 3423.
17. Wang, W.Y., Niu, X.L., Gao, Y.C., et al., *Cryst. Growth Des.*, 2010, vol. 10, p. 4050.
18. Zhang, F.W., Li, Z.F., Ge, T.Z., et al., *Inorg. Chem.*, 2010, vol. 49, p. 3776.
19. Feng, X., Miao, S.B., Li, T.F., and Wang, L.Y., *Russ. J. Coord. Chem.*, 2011, vol. 37, p. 572. doi 10.1134/S1070328411070050
20. Deng, J.H., Zhong, D.C., Luo, X.Z., et al., *Cryst. Growth Des.*, 2012, vol. 12, p. 4861.
21. Cai, S.L., Zheng, S.R., Wen, Z.Z., et al., *CrystEngComm*, 2012, vol. 14, p. 8236.
22. Wang, C.J., Wang, T., Li, L., et al., *Dalton Trans.*, 2013, vol. 42, p. 1715.
23. Tan, Y.H., Wu, J.S., Yang, Q.R., et al., *Polyhedron*, 2013, vol. 57, p. 24.
24. Gao, R.M., Li, J., Guo, M.W., and Li, G., *Russ. J. Coord. Chem.*, 2014, vol. 40, p. 379. doi 10.1134/S1070328414050042
25. Yang, R., Cai, S.L., Wen, Z.Z., et al., *Inorg. Chem. Commun.*, 2014, vol. 46, p. 98.
26. Zeng, R.H., Liang, J.H., Lin, L.J., et al., *Z. Anorg. Allg. Chem.*, 2015, vol. 641, p. 2677.
27. Sang, Y.L., Xin, J.F., and Gao, R.M., *Russ. J. Coord. Chem.*, 2016, vol. 42, p. 410. doi 10.1134/S1070328416050079
28. Cai, S.L., Zheng, S.R., Fan, J., et al., *CrystEngComm*, 2016, vol. 18, p. 1174.
29. Cai, S.L., He, Z.H., Wu, W.H., et al., *CrystEngComm*, 2017, vol. 19, p. 3003.
30. Cai, S.L., Zhang, K., Wang, S., et al., *Struct. Chem.*, 2017, vol. 28, p. 577.
31. Cai, S.L., Wang, S., He, Z.H., et al., *Z. Anorg. Allg. Chem.*, 2017, vol. 643, p. 593.
32. Cai, S.L., Lin, H.M., Yang, J.R., et al., *Russ. J. Coord. Chem.*, 2018, vol. 44, p. 64. doi 10.1134/S1070328418010025
33. Zheng, S.R., Cai, S.L., Pan, M., et al., *CrystEngComm*, 2011, vol. 13, p. 883.
34. Li, T.T., Cai, S.L., Zeng, R.H., et al., *Inorg. Chem. Commun.*, 2014, vol. 48, p. 40.
35. Yang, H.X., Jian, S.J., Liang, Z., et al., *Inorg. Chem. Commun.*, 2015, vol. 61, p. 57.
36. Cai, S.L., Zheng, S.R., Wen, Z.Z., et al., *Cryst. Growth Des.*, 2012, vol. 12, p. 3575.
37. Zheng, S.R., Cai, S.L., Fan, J., et al., *Inorg. Chem. Commun.*, 2011, vol. 14, p. 1097.
38. *SMART and SADABS*, Madison: Bruker AXS Inc.
39. Sheldrick, G.M., *Acta Crystallogr., Sect. A: Found. Adv.*, 2015, vol. 71, p. 3.
40. Sheldrick, G.M., *Acta Crystallogr., Sect. C: Struct. Chem.*, 2015, vol. 71, p. 3.
41. Blatov, V.A. and Shevchenko, A.P., *TOPOS 4.0*, Russia: Samara State Univ., 1999.
42. Yue, Z.F., Chen, Z.N., Zhong, Y.H., and Li, G., *J. Coord. Chem.*, 2015, vol. 68, p. 2507.
43. Lu, W.G., Jiang, L., Feng, X.L., and Lu, T.B., *Cryst. Growth Des.*, 2008, vol. 8, p. 986.